C. elegans ankyrin repeat protein VAB-19 is a component of epidermal attachment structures and is essential for epidermal morphogenesis

Mei Ding[1], Alexandr Goncharov[2], Yishi Jin[2] and Andrew D. Chisholm[1,*]

[1]Sinsheimer Laboratories, Department of Molecular, Cellular, and Developmental Biology, University of California, Santa Cruz, CA 95064, USA
[2]Howard Hughes Medical Institute, Department of Molecular, Cellular, and Developmental Biology, University of California, Santa Cruz, CA 95064, USA
*Author for correspondence (e-mail: chisholm@biology.ucsc.edu)

Accepted 11 August 2003

Development 130, 5791-5801

doi:10.1242/dev.00791

Summary

Elongation of the epidermis of the nematode *Caenorhabditis elegans* involves both actomyosin-mediated changes in lateral epidermal cell shape and body muscle attachment to dorsal and ventral epidermal cells via intermediate-filament/hemidesmosome structures. *vab-19* mutants are defective in epidermal elongation and muscle attachment to the epidermis. VAB-19 is a member of a conserved family of ankyrin repeat-containing proteins that includes the human tumor suppressor *Kank*. In epidermal cells, VAB-19::GFP localizes with components of epidermal attachment structures. In *vab-19* mutants, epidermal attachment structures form normally but do not remain localized to muscle-adjacent regions of the epidermis. VAB-19 localization requires function of the transmembrane attachment structure component Myotactin. *vab-19* mutants also display aberrant actin organization in the epidermis. Loss of function in the spectrin SMA-1 partly bypasses the requirement for VAB-19 in elongation, suggesting that VAB-19 and SMA-1/spectrin might play antagonistic roles in regulation of the actin cytoskeleton.

Key words: *C. elegans*, Epidermis, Morphogenesis, Ankyrin repeat, Spectrin

Introduction

During development, different tissues must coordinate their morphogenesis to form functional units. *Caenorhabditis elegans* offers unique experimental opportunities for the genetic analysis of morphogenesis (Chin-Sang and Chisholm, 2000; Simske and Hardin, 2001). The *C. elegans* embryo changes from being bean shaped into the long thin shape of the larva, a process known as elongation. Over a period of 4 hours, the embryo elongates from 50 μm to 250 μm along its long axis, simultaneously contracting in circumference. Elongation involves coordinated changes in the shapes of cells within the epidermis. Cell ablation experiments suggest that these shape changes occur cell autonomously and require circumferential actin microfilament bundles (CFBs) in epidermal cells (Priess and Hirsh, 1986). Analysis of elongation-defective mutants has identified epidermal proteins that regulate actin-based contractions, leading to the model that actomyosin-based contraction of lateral epidermal cells provides the driving force for epidermal cell shape change (Piekny et al., 2000; Wissmann et al., 1997; Wissmann et al., 1999). Loss of function in the SMA-1/β_H-spectrin and the SPC-1/α-spectrin results in mild disorganization of epidermal actin bundles and slower or blocked elongation (McKeown et al., 1998; Norman and Moerman, 2002), showing that epidermal actin organization is important for elongation.

During early epidermal elongation, body muscle cells migrate to positions underlying dorsal and ventral epidermis. At the same time, attachment structures begin to form in the epidermis adjacent to the muscle cells. Attachment structures were first observed using electron microscopy, and were termed fibrous organelles (Francis and Waterston, 1991; Hresko et al., 1994). Attachment structures are confined to the regions of the epidermal cells overlying muscle and some other cells, suggesting that muscle cells regulate attachment structure localization within the epidermal cytoskeleton (Hresko et al., 1994). Epidermal attachment structures form part of a molecular link between the contractile apparatus of the muscle and the cuticular exoskeleton.

Epidermal elongation is not dependent solely on cell autonomous processes in the epidermis but also requires non-autonomous function of muscle cells. Mutations that severely disrupt muscle function also block epidermal elongation soon after muscle contractions normally start, leading to the Pat (paralysed, arrested at twofold) phenotype (Barstead and Waterston, 1989; Barstead and Waterston, 1991; Gettner et al., 1995; Williams and Waterston, 1994). The requirement for muscle function in elongation remains unexplained; defective muscles might hinder epidermal cell shape changes, or muscle contraction might provide additional stretching forces on the epidermis allowing elongation beyond the twofold stage.

An alternative explanation comes from the observation that muscle cells influence the organization of attachment structures in the epidermis. Loss of embryonic attachment structure

components results in elongation defects. The spectraplakin VAB-10A is the *C. elegans* ortholog of Plectin, a conserved component of hemidesmosomes; VAB-10A is localized to attachment structures and is essential for elongation (Bosher et al., 2003). The cytoplasmic intermediate filament IFB-1A is a component of attachment structures (W.-M. Woo and A.D.C., unpublished) and is also essential for elongation beyond the twofold stage (Karabinos et al., 2001). The transmembrane protein Myotactin localizes to attachment structures and is essential for elongation; in the absence of Myotactin, attachment structures do not remain localized to muscle-adjacent regions of the epidermis, suggesting that Myotactin receives a muscle-dependent signal that anchors attachment structures (Hresko et al., 1999).

Here, we report that *vab-19* is essential for epidermal elongation and that it encodes the *C. elegans* ortholog of a tumor suppressor locus, *Kank* (Sarkar et al., 2002). A functional VAB-19 fusion with green fluorescent protein (VAB-19::GFP) localizes to epidermal attachment structures. The function of *vab-19* is not required for the assembly of attachment structures but is required for their localization to muscle-adjacent regions of epidermis. VAB-19 is also required for normal epidermal actin organization, and *vab-19* mutant phenotypes are specifically suppressed by loss of function in the β_H spectrin SMA-1. VAB-19 might antagonize the function of β_H spectrin in the apical actin cytoskeleton, permitting attachment structures to develop beyond a certain stage and allowing epidermal cells to change shape.

Materials and methods

Strains and genetics

C. elegans was grown on NGM plates as described by Brenner (Brenner, 1974). Bristol N2 was used as the wild type. *vab-19(e1036)* was isolated by J. Lewis in screens for mutants with epidermal morphogenesis defects and displays a cold-sensitive phenotype. *vab-19(ju406)* was isolated in a semiclonal screen for epidermal morphogenesis mutants (M.D., W.-M. Woo and A.D.C., unpublished). EMS-mutagenized hermaphrodites were allowed to self-fertilize and two F_1 progeny were put on a single plate as a semiclone. The F_2 progeny of each semiclone were examined for the segregation of dead larvae resembling *e1036*. Siblings then were recovered to produce progeny. 8000 mutagenized genomes were screened.

Four-dimensional microscopy

We made four-dimensional movies as previously described (Chin-Sang et al., 1999). We recorded movies from ten *vab-19(e1036*cs*)* embryos (progeny of parents shifted to 15°C as L4s), eight *vab-19(ju406)* and five *vab-19(ju406)/nDf2* embryos. All *vab-19* mutant embryos arrested at the twofold stage.

Molecular cloning of *vab-19*

The *vab-19(e1036)* mutation was genetically mapped to the *lin-42 sup-9* interval on the left arm of chromosome II (map data are available from Wormbase). The chromosomal deficiencies *nDf2* and *nDf3* fail to complement *vab-19*. Cosmids were obtained from the Sanger Institute (Hinxton, UK). DNA preparation and subcloning followed standard procedures (Sambrook and Russell, 2001).

In rescue experiments, we assayed rescue of the *vab-19* lethal phenotypes and of the Vab phenotypes of *e1036* animals raised at a semipermissive temperature. Rescue of lethal phenotypes was scored qualitatively (growth or no growth of the transgenic strain at 15°C). Rescue of Vab phenotypes was scored in Rol animals; over 1000 animals were scored for each array tested. At 20°C, 20% of *vab-19(e1036)* animals are Vab; rescue was defined as a statistically significant reduction in the proportion of Vab in Rol animals.

Initial transformation experiments showed that cosmid F42G2 contained partial *vab-19* rescuing activity; the *vab-19* exons contained in F42G2 encode the N-terminal 484 amino acids of VAB-19. The minimal genomic fragment that fully rescues *vab-19* phenotypes is contained in clone pCZ440, made by ligating a 6.6 kb *Mlu*I-*Xba*I fragment from cosmid F42G2 with a 6.5 kb *Mlu*I-*Sal*I fragment of cosmid K02G6. *vab-19* corresponds to Wormbase gene model T22D2.1. cDNAs for *vab-19* had been isolated in a genome-wide expressed sequence tag project (Maeda et al., 2001). The longest cDNA, yk481c2, was sequenced completely and found to lack the first seven bases of the predicted coding sequence. In the process of allele sequencing, we also identified one error in the published genomic sequence, which changes one predicted intron to an exon. The predicted *vab-19* gene structure between residues 470 and 504 was confirmed by sequencing yk481c2 and another cDNA, yk656c2. The 6.5 kb *Mlu*I-*Sal*I genomic DNA fragment in pCZ440 was replaced with the corresponding cDNA fragment from yk481c2 to make a *vab-19* minigene (pCZ437). To make the VAB-19::GFP fusion construct pCZ441, GFP coding sequence from pPD113.37 (Fire lab vector kit) was inserted in frame at the *Bam*HI site of pCZ437.

To identify lesions in *vab-19* alleles, *vab-19* genomic DNA (including all exons and exon-intron junctions) was amplified from *vab-19* mutant and wild-type animals. DNA sequences were determined using ^{33}P-labeled primers and the *fmol* sequencing kit (Promega). All lesions were confirmed on both strands and from DNAs prepared in independent polymerase chain reactions (PCRs). Sequences of primers used are available on request.

To determine the effect of the *ju406* mutation on *vab-19* splicing, reverse-transcription PCR (RT-PCR) was performed on total RNA isolated from *vab-19(ju406)* animals (primer sequences available on request). We sequenced 13 RT-PCR products and found two kinds of mutant transcript containing frame shifts and premature stop codons in exons 3 or 4.

Germ-line transformation

Germ-line transformation followed standard procedures (Mello et al., 1991) using 5-10 ng μl^{-1} of *vab-19* DNA and 50 ng μl^{-1} pRF4 coinjection marker. In all transgenic analysis, at least five independent lines were scored. Integrants of functional VAB-19::GFP arrays were obtained by TMP-UV mutagenesis. Five independent integrants of VAB-19::GFP (*juIs167*, *juIs168*, *juIs169*, *juIs170* and *juIs171*) were identified and backcrossed multiple times before data collection. The VAB-19::GFP transgenes displayed identical expression patterns and rescue of *vab-19* phenotypes. *juIs167* was used in Figs 3-5, and *juIs169* was used in Fig. 6.

Immunofluorescence and phalloidin staining

Whole mount immunofluorescence staining was performed following the protocol of Finney and Ruvkun (Finney and Ruvkun, 1990). To analyse VAB-19::GFP in embryos, Clorox-treated animals were fixed in 1% paraformaldehyde for 3.5 hours on ice and incubated with anti-GFP antibodies (Chemicon) at 1:100 dilution and appropriate secondary antibodies. MH4 and MH46 (Developmental Hybridoma Studies Bank, University of Iowa) were used at 1:300 dilution. Images were collected using a Leica TCS-NT Confocal microscope. VAB-19::GFP expression was observed using a Zeiss Axioskop equipped with a HQ-FITC filter (Chroma). Phalloidin staining was performed as described by Costa et al. (Costa et al., 1997). Embryos were dislodged from NGM plates. After rinsing in M9 buffer, the eggshells were digested for 10 minutes using chitinase (Sigma). Embryos were fixed for 20 minutes in 4% paraformaldehyde, washed in PBS and stained for 1 hour with 0.3 μM phalloidin labeled with Alexa Fluor 488 (Molecular Probes).

Electron microscopy

L1 animals were processed for electron microscopy as previously described (Hallam et al., 2002). Serial thin sections were taken from three wild-type L1s and two *vab-19(e1036)* L1s; the *vab-19* mutants were progeny of parents that had been shifted to 15°C at the L4 stage. The wild-type sections are longitudinal sections from the head region.

Results

vab-19 mutants display defects in epidermal morphogenesis

The *vab-19* gene is defined by two mutant alleles, *e1036*cs and *ju406*. At permissive temperatures (22.5°C), about 90% of *e1036* animals survive to adulthood and display variable defects in epidermal morphology (the Vab phenotype). At restrictive temperatures (15°C), all *e1036* mutants arrest at the twofold stage of embryonic elongation (Fig. 1H). The phenotypes of *e1036/Df* animals and *e1036/e1036* animals raised at 15°C were indistinguishable, suggesting that *e1036* causes complete loss of function at 15°C. In all studies of mutant phenotypes described below, *ju406* behaved indistinguishably from *e1036* at 15°C.

To determine more precisely the role of *vab-19* in embryonic morphogenesis, we analysed *vab-19* mutant embryos using time-lapse Nomarski microscopy and found that *vab-19* mutant embryos display defects in epidermal elongation. Wild-type embryos begin to elongate at ~350 minutes after first cleavage and elongate three- to fourfold by the time of hatching (at 800 minutes). At the 1.75-fold stage (~430 minutes), body wall muscle contractions begin and the embryos start to twitch weakly. By the twofold stage (~450 minutes), the embryos roll vigorously and continue their elongation until threefold (~520 minutes, Fig. 1C). *vab-19* mutant embryos displayed normal elongation prior to the twofold stage (Fig. 1E,F). Within 10-20 minutes of reaching the twofold stage, *vab-19* mutant embryos stopped elongating (Fig. 1G). *vab-19* embryos also displayed detachment of body muscles from the epidermis (Fig. 1H, arrowhead; Fig. 1I,J). Consistent with a gradual failure of muscle attachments, *vab-19* mutant embryos twitched normally but never rolled, and were essentially paralysed after the twofold stage. Development continued, as indicated by cuticle formation and development of a pharynx, and most *vab-19* embryos hatched a few hours later than the wild type, although they did not grow after hatching. In general, the *vab-*

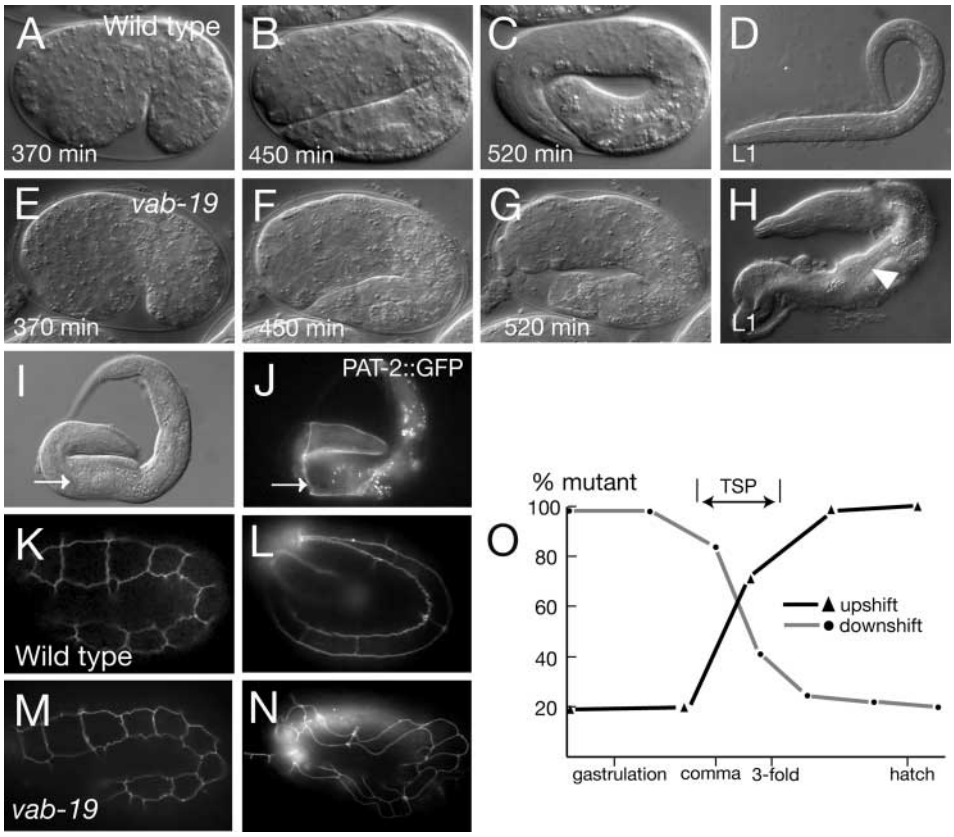

Fig. 1. *vab-19* mutants are defective in embryonic morphogenesis and muscle attachment. (A-H) Frames from time-lapse Nomarski movies of wild-type and *vab-19(ju406)* embryos. *vab-19* mutant embryos appear normal at comma stage and twofold stage (E,F). 70 minutes after the twofold stage, the wild-type embryo has elongated to the threefold stage (C), whereas the *vab-19* mutants have stopped elongation and show constrictions and lumps in the epidermis (G). *vab-19* mutants typically hatch as deformed L1 stage animals with extensive muscle detachment (H, arrowhead; I,J, arrow). (K-N) Epidermal junctions visualized by AJM-1::GFP in wild-type and *vab-19* embryos at 1.75-fold (K,M) and post-twofold stages (L,N), showing that epidermal adherens junctions form normally in *vab-19* mutants. (O) The *vab-19(e1036*cs*)* temperature-sensitive period (TSP) is during early elongation. The *x* axis represents developmental stages at which embryos were up- or down-shifted. The *y* axis represents the proportion of embryos that showed *vab-19* lethal and Vab phenotypes at 22.5°C. At least 24 embryos were scored for each time point. Up-shift involved transferring embryos raised at 15°C to 22.5°C, whereas down-shift involved transferring embryos raised at 22.5°C to 15°C. The midpoint of the TSP is between the 1.5-fold and twofold stages.

19 phenotype resembles the 'weak Pat' phenotype described by Williams and Waterston (Williams and Waterston, 1994). Expression of the adherens junction marker AJM-1 (Koppen et al., 2001) in *vab-19* mutants was similar to the wild type (compare Fig. 1M,N with 1K,L), showing that epidermal cells are specified correctly and have normal cell-cell contacts.

Although our analysis did not reveal defects earlier than elongation in *vab-19* mutants, we could not rule out the possibility that lack of VAB-19 causes defects in early development and that these defects indirectly affect elongation. To address this question, we performed temperature shift experiments using the cold-sensitive allele *e1036*. When *vab-19(e1036)* embryos grown at 22.5°C were shifted to 15°C before elongation, almost 100% of these embryos arrested at the twofold stage. When *vab-19(e1036)* embryos grown at 15°C were shifted to 22.5°C before elongation, about 80% of these animals survived to adulthood and appeared wild type in morphology (Fig. 1O). Thus, these experiments identify a *vab-19* temperature-sensitive period at the twofold stage of elongation, suggesting that VAB-19 function is directly involved in epidermal elongation.

VAB-19 is a member of a conserved ankyrin repeat-containing protein family

We mapped *vab-19* between *lin-42* and *sup-9* on the left arm of chromosome II, and tested genomic DNA clones from this region for their ability to rescue *vab-19(e1036)* phenotypes in transgenic lines (Fig. 2A). *vab-19* phenotypes were partly rescued by cosmid F42G2. Further rescue analysis showed that *vab-19* corresponds to the gene T22D2.1 (see Materials and methods).

The predicted VAB-19 protein is a member of a conserved protein family containing four ankyrin repeats in their C-termini (VAB-19 residues N863-T999; Fig. 2B). The *Drosophila* genome contains a single VAB-19 ortholog, CG10249. The human genome contains two orthologs, KIAA1518 and KIAA0172/*Kank*, and the mouse and rat genomes each contain two VAB-19-related genes. The cellular

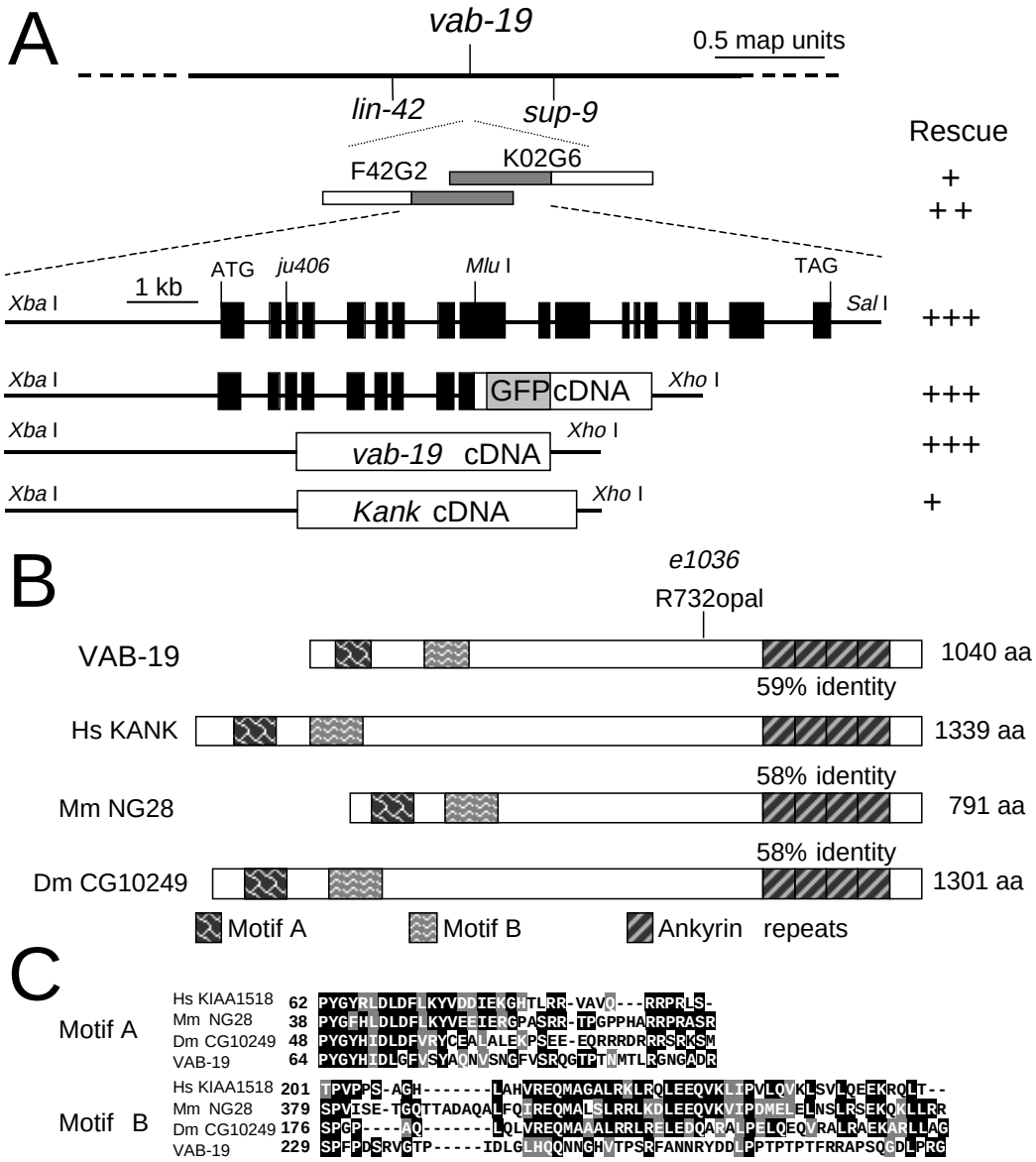

Fig. 2. The *vab-19* gene encodes a conserved ankyrin repeat-containing protein. (A) Genetic and physical maps of the *vab-19* region and structure of the *vab-19* gene. All rescue experiments used *vab-19(e1036)* and the *rol-6* (pRF4) co-injection marker. Initial experiments assayed rescue of the morphological defects of *e1036* at the semipermissive temperature 22.5°C. Rescue was classified as follows: no rescue (injection of pRF4 alone) means that 20% of Rol animals are Vab; weak rescue (+) means that 5-10% Rol animals are Vab; partial rescue (++) means that 2-5% Rol animals are Vab; full rescue (+++) means that <2% animals are Vab. All rescuing transgenes also rescue the lethal Vab-19 phenotypes. (B) Comparison of *C. elegans* VAB-19, human Kank/KIAA0172, mouse NG28 and *Drosophila* CG10249, isoform C. A second murine VAB-19 homolog is represented by an apparent partial sequence (AAH06647, not shown). The predicted effects of *vab-19* mutations are indicated. The four ankyrin repeats are shown as striped boxes. Sequence alignments suggest that the four highly conserved repeats might be flanked by partial or divergent ankyrin repeats (not shown). (C) ClustalW alignments of VAB-19 family N-terminal motifs A and B.

functions of these VAB-19 family members have not been determined. The KIAA0172 gene, also known as *Kank*, is downregulated in renal cell carcinomas, suggesting that it acts as a tumor suppressor (Sarkar et al., 2002). Within the ankyrin repeats, *C. elegans* VAB-19 is 59% identical to human Kank and 58% identical to *Drosophila* VAB-19 (Fig. 2B). Alignments of VAB-19 family members also revealed two short regions of conservation in the N-terminus (Fig. 2C). These motifs appear to be unique to the VAB-19 family and are termed motif A (VAB-19 residues P64-R103) and motif B (VAB-19 residues S229-G285). Expression of the human *Kank* cDNA under the control of the *vab-19* promoter partly rescued *vab-19* mutant phenotypes (Fig. 2A), suggesting that VAB-19 and Kank have similar cellular roles.

We determined the molecular lesions of *vab-19* alleles. *ju406* alters the exon 3 splice acceptor (tccag|AAA to tccaa|AAA); *vab-19(ju406)* animals express aberrantly spliced transcripts that encode truncated proteins (see Materials and methods). The cold-sensitive allele *e1036* results in a premature stop codon (R732opal) before the ankyrin repeat domain. *e1036* behaves genetically as a null at 15°C and as a hypomorph at higher temperatures. At the restrictive temperature, *e1036* appears to make the mRNA unstable and subject to nonsense-mediated decay by the SMG system (Mango, 2001), because the lethal and Vab phenotypes of *e1036* were almost completely suppressed by a mutation in *smg-3* (Table 1); *smg-3* did not suppress *ju406* (data not shown). *vab-19(e1036)* might retain partial function owing to read-through of the stop codon at the permissive temperature or in a *smg* background; alternatively, truncated proteins made in *e1036* might themselves be cold sensitive.

VAB-19 localization is dynamic during embryonic epidermal morphogenesis

To determine how *vab-19* might function in vivo, we generated reporter constructs containing translational fusions of the full-length *vab-19* coding sequence to GFP. These VAB-19::GFP constructs completely rescued *vab-19* null mutant phenotypes (Fig. 2), suggesting that they reflect the endogenous VAB-19 expression pattern. VAB-19::GFP was first detected in embryos at the onset of elongation (Fig. 3A). At this stage, VAB-19::GFP localization was diffuse in dorsal and ventral, but not in lateral, epidermal cells. During early elongation, VAB-19::GFP started to accumulate in muscle-adjacent regions of dorsal and ventral epidermal cells (Fig. 3B, arrow). During intermediate stages of elongation, VAB-19::GFP became localized to the parts of the epidermis adjacent to body wall muscles (Fig. 3C). Finally, during the late elongation, larval and adult stages, VAB-19::GFP localized to circumferential bands in epidermis adjacent to muscles (Fig. 3D-F) and to mechanosensory neuron processes (not shown). Within these regions, the pattern of circumferential bands is interrupted by gaps where other neuronal processes intervene between muscles and the epidermis (e.g. Fig. 3F). This pattern of localization of VAB-19::GFP resembles that of epidermal attachment structures. Furthermore, transgenes containing the VAB-19 cDNA under the control of the *ajm-1* promoter, which is expressed in the epidermis and other epithelial tissues but not in muscles (Köppen et al., 2001), also fully rescued *vab-19* phenotypes (not shown), consistent with VAB-19 functioning in epidermal cells.

Table 1. Quantification of *vab-19* phenotypes and suppression by *sma-1*

Genotype	Temperature (°C)	Percent lethal
vab-19(e1036cs)	15	100
vab-19(e1036cs)	20	43.0
vab-19(e1036cs)	22.5	11.0
vab-19(ju406)	20	100
smg-3(r867) vab-19(e1036cs)	15	10.0
vab-19(e1036cs) sma-1(e30)	20	13.7
vab-19(e1036cs) sma-1(e30)	15	51.5
vab-19(e1036cs) sma-1(ru18)	15	43.4
vab-19(ju406) sma-1(e30)	20	41.0
vab-19(ju406) sma-1(ru18)	20	45.5

The penetrance of lethal phenotypes (combined embryonic and larval lethality) was quantified as described in Materials and methods. *sma-1* mutants display less than 5% lethality (McKeown et al., 1998).

To determine whether VAB-19 is a component of epidermal attachment structures, we asked whether VAB-19::GFP localized with known components of attachment structures. Attachment structures contain several intermediate filament (IF) proteins, some of which are recognized by monoclonal antibody MH4 (Francis and Waterston, 1991). During early elongation, MH4 staining accumulated in a single patch in dorsal epidermal cells (Fig. 4B), whereas VAB-19::GFP remained diffuse (Fig. 4A). During the intermediate elongation stage, VAB-19::GFP and MH4 staining displayed more extensive colocalization (Fig. 4D-F). During later elongation and afterwards, VAB-19::GFP and MH4 staining fully co-localized to circumferential bands (Fig. 4G-L). Because MH4-positive IFs become localized before VAB-19::GFP, VAB-19 probably is not required for the initial recruitment of IFs to attachment structures.

The transmembrane protein Myotactin maintains localization of attachment structures to muscle-adjacent parts of the epidermis (Francis and Waterston, 1991; Hresko et al., 1999). Myotactin itself initially localizes to muscle-adjacent regions of the epidermis and later becomes organized into attachment structures. VAB-19::GFP colocalized with Myotactin before the twofold stage (Fig. 4M-O). Both Myotactin and VAB-19::GFP localized to circumferential bands (Fig. 4P-R). These bands are interrupted by gaps where neuronal processes intervene between muscle and epidermis (Fig. 4J,P,Q, arrows). In contrast to Myotactin or VAB-19::GFP, MH4 staining is present or enhanced at such positions (Fig. 4K, arrow). These differences suggest that VAB-19 does not colocalize with all epidermal IFs but only those associated with muscle adjacent attachment structures.

VAB-19::GFP was also expressed in pharyngeal marginal cells, which contain prominent tonofilament-like attachment structures (Albertson and Thomson, 1976). Pharyngeal attachment structures resemble epidermal attachment structures in both ultrastructure and molecular composition, because they contain MH4-positive IFs, VAB-10A and Myotactin (Francis and Waterston, 1991). In contrast to Myotactin, which is localized to the outer basal surface of marginal cells (Fig. 4T), VAB-19::GFP was localized throughout the apical-basal axis, although it was concentrated at the apical and basal surfaces (Fig. 4S, arrow; compare with Fig. 4U). Thus, in pharyngeal marginal cells, VAB-19 might

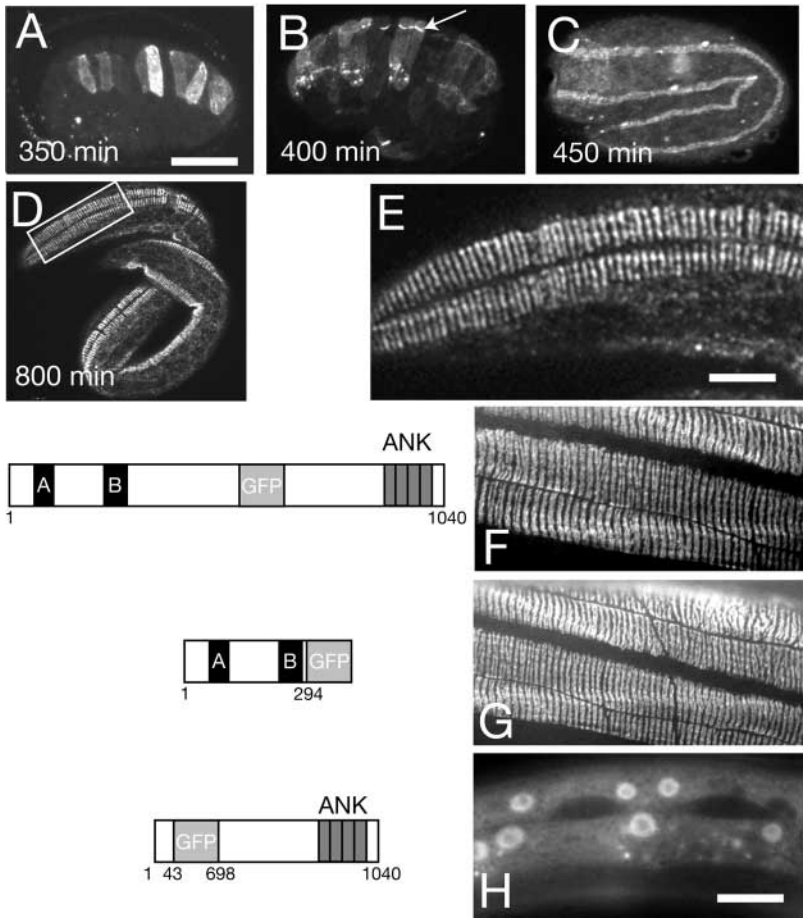

Fig. 3. VAB-19::GFP localization to epidermal attachment structures. Because the endogenous VAB-19::GFP fluorescence signal is weak, we used anti-GFP antibodies to visualize VAB-19::GFP expression. (A) At comma stage, VAB-19::GFP was diffusely expressed in dorsal epidermal cells; the uneven expression might reflect differential onset of VAB-19 expression in different cells. (B) During early elongation (1.5-fold), the VAB-19::GFP signal began to accumulate in the regions within dorsal epidermal cells that contact body muscles (arrow). (C) During the intermediate stage of elongation (1.75-fold), VAB-19::GFP mostly localized to epidermal regions adjacent to body wall muscle. (D) During later elongation (threefold stage), VAB-19::GFP was organized in circumferential bands in muscle-adjacent epidermis. Inset (E), higher magnification of the VAB-19::GFP pattern at the threefold stage. (F) In adult epidermal cells, the full length VAB-19::GFP protein is localized to attachment structures. GFP fusions to VAB-19 N-terminal fragments containing residues 1-684 (not shown) or 1-294 (G) display subcellular localization identical to that of the full-length protein. (H) GFP fusions to the VAB-19 ankyrin repeat-containing domain (residues 1-43 and 697-1040) were not localized within epidermal cells. None of the truncated protein constructs rescued *vab-19* mutant phenotypes; transgenes containing VAB-19(1-294)::GFP conferred a weak Vab phenotype in a wild-type background. Scale bars, 10 μm.

be a component of the ends of IF-containing attachment structures.

To examine how VAB-19 becomes localized to epidermal attachment structures, we fused GFP to different portions of VAB-19 and expressed these truncated proteins under the control of the *vab-19* promoter. Truncated proteins lacking the ankyrin repeats were localized normally (Fig. 3G). By contrast, a truncated protein lacking the N-terminal domain was diffusely localized in dorsal and ventral epidermal cells (Fig. 3H). Thus, the VAB-19 N-terminal domain, containing the conserved motifs A and B, might be both necessary and sufficient for localization of VAB-19. GFP-tagged fusion proteins containing only motif A or only motif B were diffusely expressed (not shown), suggesting that both motifs are required together for normal VAB-19 localization.

Initial development of epidermal attachments is normal in *vab-19* mutants

Because, during later stages of embryogenesis, VAB-19 localizes in or close to attachment structures, we examined the effect of *vab-19* mutations on the localization of other attachment structure components. One of the first proteins to become localized to attachment structures is VAB-10A, a *C. elegans* spectraplakin orthologous to Plectin and *Drosophila* Shot (Bosher et al., 2003). During early and intermediate (twofold) stages of epidermal elongation, the localization of intermediate filaments (MH4) and VAB-10A appeared normal in *vab-19* mutants (Fig. 5). However, during later elongation, IFs or VAB-10A became delocalized, expanding into regions not adjacent to body wall muscle, yet remaining in regular circumferential bands (compare Fig. 5C and 5F for MH4 staining). Thus, VAB-19 is a component of attachment structures but is not essential for their formation.

Because of the similarities between VAB-19 and Myotactin distribution, we also analysed the localization of Myotactin in *vab-19* mutants. Myotactin staining appeared normal in 1.5-fold and twofold *vab-19* embryos (Fig. 5). However, in *vab-19* mutants, Myotactin never became localized into circumferential stripes and instead remained localized to longitudinal bands in muscle-adjacent regions of the epidermis (compare Fig. 5I and 5M). Thus, VAB-19 is required to recruit Myotactin to attachment structures but not for its localization to muscle-adjacent regions.

To learn whether VAB-19 is required for aspects of attachment structure morphology not discernible by immunostaining, we used electron microscopy to compare attachment structures in wild-type and *vab-19* mutant L1s. Attachment structures were present in *vab-19* mutants and were correctly distributed with respect to actin bundles, as judged by the registration of attachment structures and cuticle annuli (which form directly above actin CFBs) in longitudinal sections (Fig. 5O and inset). The epidermis appears thicker in *vab-19* mutants and attachment structures are extended, possibly because of the reduced length of the animal. Thus, VAB-19 is not essential for the correct distribution of attachment structures with respect to actin CFBs.

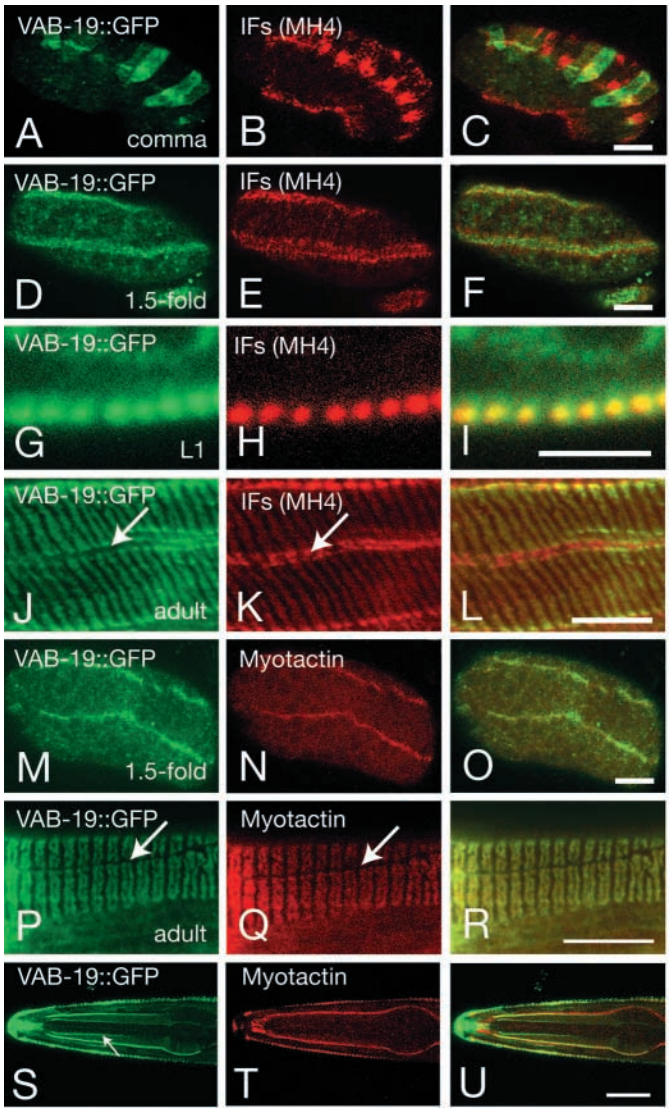

Fig. 4. VAB-19 localizes to epidermal attachment structures. (A-I) VAB-19::GFP progressively co-localizes with intermediate filaments. Confocal images of VAB-19::GFP expression (*juIs167*) visualized using anti-GFP immunostaining (green); intermediate filaments were visualized using the MH4 monoclonal antibody (red). At the comma stage (A-C), VAB-19::GFP partly colocalized with intermediate filaments. At the intermediate elongation stage (D-F), VAB-19::GFP and intermediate filaments both localized to muscle-adjacent regions of the dorsal and ventral epidermis. During later embryogenesis and larval stages until adulthood, staining of anti-GFP and MH4 was coincident. (G-I) L1 stage epidermis in z-axis section. (J-L) Lateral view of adult epidermis. (M-R) Colocalization of VAB-19::GFP and Myotactin (MH46 antigen). At the intermediate elongation stage (M-O), VAB-19::GFP and Myotactin are both localized to epidermal cell regions adjacent to muscle. In adults (P-R), the bands of Myotactin and VAB-19::GFP are interrupted by gaps corresponding to the positions of neuronal processes (arrows), at which positions MH4 staining is usually enhanced (K, arrow). Like Myotactin, but unlike MH4 staining, VAB-19::GFP is absent from such process gaps (compare J and P). VAB-19::GFP was also expressed in pharyngeal marginal cells (S); unlike Myotactin (T), VAB-19::GFP was localized throughout the apical basal axis of these cells and was more concentrated at the apical and basal surfaces. Scale bars: 5 μm (G-I); 10 μm (all others).

We asked whether attachment structure components were required for VAB-19 localization by introducing VAB-19::GFP into animals lacking Myotactin or VAB-10A. In Myotactin (*let-805*) mutants, VAB-19::GFP was normally localized to muscle-adjacent regions of the epidermis but never became distributed into circumferential stripes. Within 15-20 minutes of muscle contraction starting (~430 minutes), VAB-19::GFP became dispersed into puncta within epidermal cells (Fig. 6B). Thus, VAB-19 requires Myotactin for its subcellular localization in epidermal cells. By contrast, in *vab-10A(ju281*ts*)* mutants, VAB-19::GFP remained confined to the regions of epidermal cells overlying muscle (Fig. 6D) but never became localized to attachment structures. Thus, neither Myotactin nor VAB-10A is required for VAB-19 to become localized adjacent to muscles but both are required for VAB-19 to be recruited to attachment structures.

Disorganization of the actin cytoskeleton in *vab-19* mutants can be suppressed by reduction in spectrin function

The driving force for epidermal elongation is provided by contraction of circumferential actin bundles (CFBs) (Priess and Hirsh, 1986). Because *vab-19* mutants have defects in elongation, we asked whether VAB-19 is required for normal actin distribution. During elongation, actin CFBs are circumferentially oriented in the epidermis (Fig. 7A-D). Actin distribution in *vab-19* mutants appeared normal until the 1.5-fold stage (Fig. 7E). As the mutant embryos developed to the twofold stage, the epidermal actin cytoskeleton became disorganized. For example, actin bundles were absent or reduced from apical epidermis (Fig. 7F, arrow). Actin CFBs were often misoriented or splayed (Fig. 7G,H). Although some of these actin bundles might represent misplaced actin from other parts of the epidermis, the apical CFBs constitute the most prominent actin structures in the epidermis at this stage. The disorganization of actin bundles was usually more obvious where body muscles had detached from epidermal cells. This result suggests that muscle detachment might result in the disorganization of actin bundles, which then blocks epidermal elongation.

To determine whether VAB-19 displayed interactions with other components of the apical actin cytoskeleton we tested for genetic interactions between *vab-19* and other genes required for normal elongation. The SMA-1 β_H spectrin is required for organization of the actin cytoskeleton within the epidermis (McKeown et al., 1998). Mutants in *sma-1* are viable yet elongate more slowly than the wild type. We found that loss of *sma-1* function strongly suppressed the elongation arrest and lethal phenotypes of *vab-19* mutants (Table 1). Viable *vab-19 sma-1* double mutants were indistinguishable from *sma-1* mutants in both elongation rate and terminal phenotype (data not shown). Multiple alleles of *sma-1* suppressed both alleles of *vab-19*. By contrast, *sma-1* mutations did not suppress the phenotypes of other attachment structure or epidermal elongation mutants including *vab-10A*/Plectin, *vab-10B*/MACF, *pat-3*/β-integrin, *let-805*/Myotactin and *mup-4* (data not shown). The gene-specific suppression of *vab-19* by *sma-1* suggests that VAB-19 and SMA-1 have antagonistic functions. The expression level of SMA-1 protein appeared normal in *vab-19* mutants (data not shown), suggesting that these proteins antagonize at the level of function but not

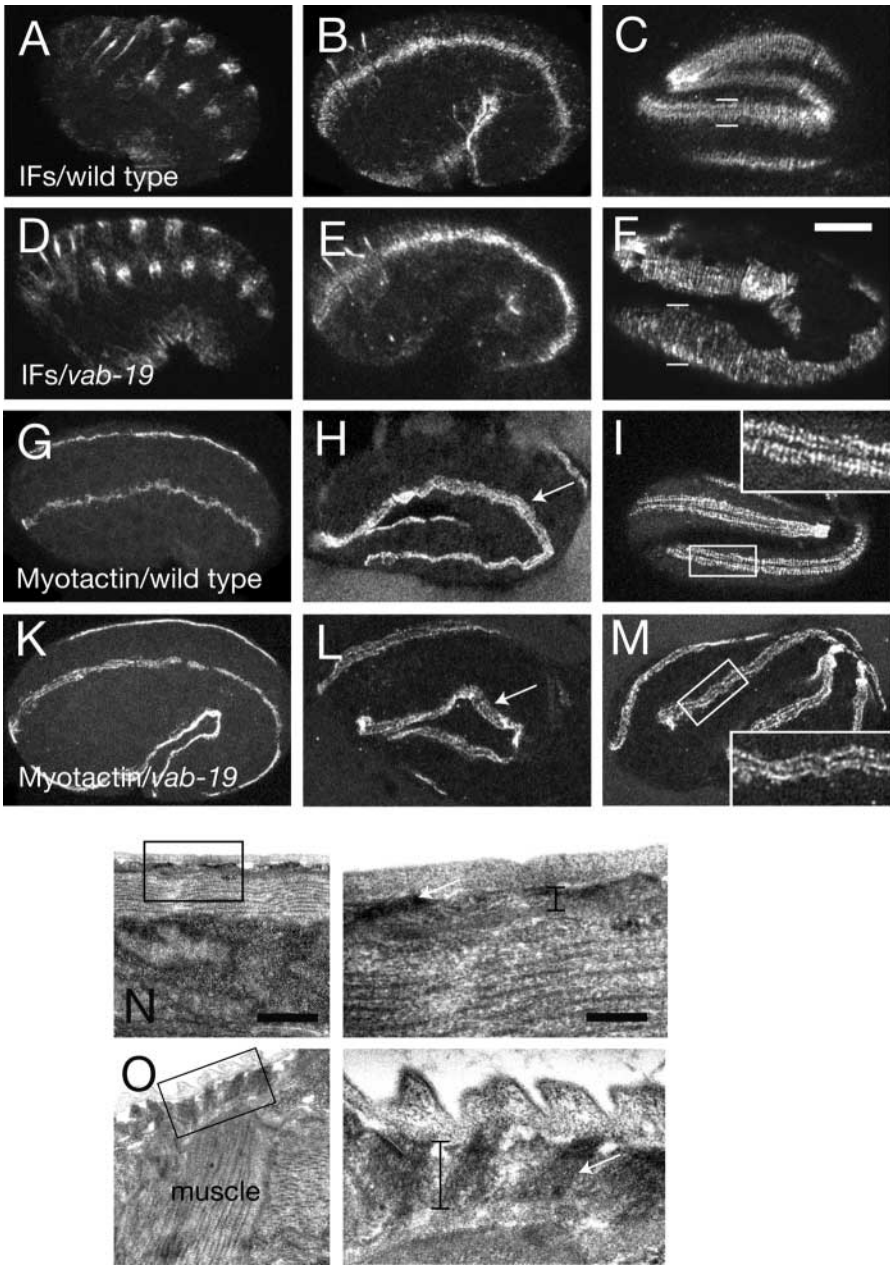

Fig. 5. Attachment structures and attachment structure components in *vab-19* mutants. (A-F) Localization of intermediate filaments (MH4 immunostaining) in the wild type and in *vab-19* mutants. (A) During early elongation in the wild type, IFs accumulate in each epidermal cell adjacent to one muscle quadrant. By the 1.5-fold stage, IFs were organized in circumferential bands in regions of epidermis adjacent to muscle, although these bands are not as regular as in later stages. (C) After the twofold stage, IFs localize to regularly spaced bands. (D-F) In *vab-19* mutants, IF staining appears normal until after the twofold stage, when it expands into regions of epidermal cells that do not overlap muscle, compared with the wild type (brackets). (G-M) Myotactin expression (visualized using the MH46 antibody) in wild-type and *vab-19* embryos. During early (comma to 1.5-fold; G,K) and intermediate (twofold; H,L) elongation stages, Myotactin appears normal in *vab-19* mutants. In wild-type threefold-stage embryos, Myotactin localizes to circumferential bands in muscle-adjacent regions of the epidermis (I, inset). In *vab-19* mutants, Myotactin is still localized to muscle-adjacent regions but remains in longitudinal rows rather than circumferential bands (M, inset). Scale bars, 10 μm. Electron microscopy (longitudinal sections) of attachment structures in wild-type L1 larva and *vab-19(e1036)* arrested larvae. In the wild type (N), attachment structures are confined to epidermis in muscle-adjacent regions, which is ~200 nm thick. In *vab-19* mutants (O), attachment structures are present and in phase with cuticle annuli but can be longer than normal. Scale bar, 500 nm (N), 150 nm (insets).

expression. Epidermal actin distribution in *vab-19 sma-1* double mutants resembled the mildly disorganized pattern of *sma-1* mutants rather than that of *vab-19* mutants (Fig. 7I,J), suggesting that the antagonism of VAB-19 and SMA-1 occurs at the level of their effects on actin distribution.

Discussion

The *vab-19* gene encodes an ankyrin repeat-domain-containing protein essential for *C. elegans* epidermal morphogenesis. The *vab-19* mutant phenotype resembles that caused by loss of function in epidermal components of attachment structures. VAB-19 is produced in the epidermis and localizes to attachment structures. VAB-19 is not essential for the formation of attachment structures but is necessary for their later localization to muscle-adjacent regions of the epidermis. VAB-19 is also necessary for the normal organization of epidermal actin. We hypothesize that VAB-19 participates in cross-talk between IF-containing attachment structures and the actin cytoskeleton.

VAB-19 is a member of a conserved protein family and is a component of *C. elegans* epidermal attachment structures

Analysis of VAB-19 homologs in *Drosophila* and vertebrates has shown that the VAB-19 family is defined by a highly conserved C-terminal domain containing four ankyrin (ANK) repeats, and a less well conserved N-terminal domain containing two novel motifs. ANK repeats are found in many proteins with diverse functions; according to the protein families database Pfam (Bateman et al., 2002), over 112 *C. elegans* proteins are predicted to contain ANK repeats. The

ANK repeat domains of VAB-19 family members are 58-60% identical to each other; outside the VAB-19 family, the closest ANK repeats (37% identity) are from zebrafish Diversin (Schwarz-Romond et al., 2002), which shares no other similarities with VAB-19. ANK repeats function as protein-protein interaction interfaces (Sedgwick and Smerdon, 1999). The high degree of conservation in the ANK repeats suggests that VAB-19 family members bind one or more conserved proteins via this domain.

The ANK-repeat domain of VAB-19 is neither necessary nor sufficient for the normal subcellular localization of the protein, as assayed using GFP fusion proteins. By contrast, two conserved motifs at the N-terminus are necessary and sufficient for VAB-19::GFP subcellular localization to attachment structures. The N-terminus of VAB-19 shows no similarity to IF-associated proteins, suggesting that VAB-19 is localized indirectly to IF-containing structures. Three non-IF proteins are found in embryonic attachment structures – the spectraplakin VAB-10A and the transmembrane receptors Myotactin and MUP-4. Our molecular epistasis experiments suggest that the final localization of VAB-19 requires both VAB-10A and Myotactin. VAB-10A is required for VAB-19 localization to attachment structures but not to muscle-adjacent regions; by contrast, Myotactin is required for both aspects of VAB-19 localization. These proteins might direct VAB-19 localization via the VAB-19 N-terminal motifs.

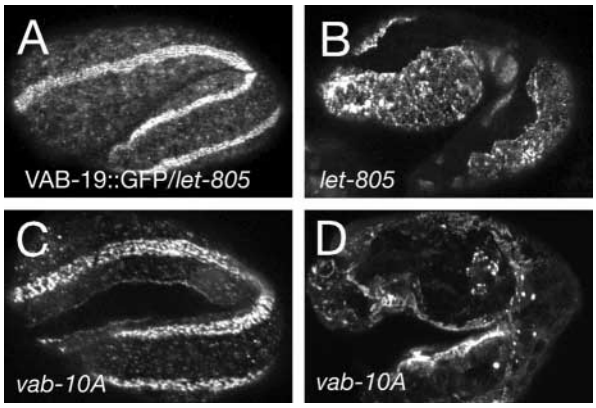

Fig. 6. VAB-19 localization is dependent on VAB-10A/Plectin and Myotactin. VAB-19::GFP localization in attachment structure mutants examined using anti-GFP immunostaining. In *let-805* (Myotactin) mutants, VAB-19::GFP localization is normal in early (1.5- to twofold stage) embryos (A); soon after the twofold stage, VAB-19::GFP dispersed into puncta throughout the dorsal and ventral epidermis (B). Live analysis of VAB-19::GFP in *let-805* mutants revealed that this delocalization occurs within 15-20 minutes of the twofold stage (not shown). In *vab-10A(ju281*ts*)* animals grown at 25°C, VAB-19::GFP localization is normal at the 1.75-fold stage (C) but becomes disorganized after the twofold stage (D). Scale bar, 10 μm.

Role of VAB-19 in development of attachment structures

Using molecular epistasis, we have explored the functional relationships between VAB-19 and other components of attachment structures. In *vab-19* mutants, the localization of known attachment structure components (IFs/MH4 and VAB-10A/Plectin) appears normal until late in embryogenesis. At this point, attachment structures redistribute into non-muscle-adjacent regions in the epidermis, although they remain in regular circumferential bands (Fig. 5F), suggesting that trans-

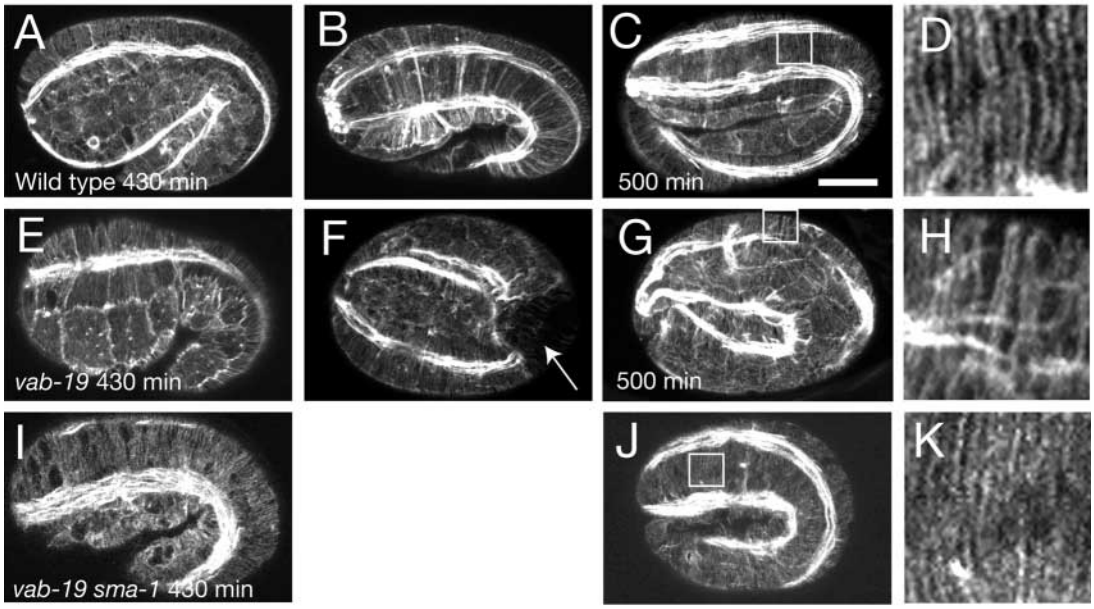

Fig. 7. Disorganization of actin filaments in *vab-19* and genetic suppression in *vab-19 sma-1* double mutants. Confocal images of F-actin distribution in wild-type and *vab-19* embryo, visualized with fluorescently labeled phalloidin. In all panels, the bright longitudinal strips of phalloidin staining correspond to body wall muscles. (A-D) In the wild type, actin filaments form parallel bundles circumferentially around the embryo. In *vab-19* embryos, actin bundles form normally at early elongation stage (E) but are more randomly oriented in later elongation (F-H) or missing from the apical surface of the epidermis (F). The disorganization of actin bundles is more obvious in regions where muscle is detached from epidermal cells (F). In *sma-1(e30);vab-19(ju406)* double mutants (I-K), actin bundles are less disorganized than in *vab-19* single mutants. Scale bar, 10 μm.

epidermal attachments initially assemble normally but, in the absence of VAB-19, they lose their normal association with muscle cells. Consistent with this interpretation, our ultrastructural analysis has shown that attachment structures are present and correctly placed with respect to cuticular structures in *vab-19* mutants.

Like VAB-19, Myotactin anchors attachment structures to muscle-adjacent regions (Hresko et al., 1999). Myotactin and VAB-19 are mutually required for their correct final localization. Myotactin's early localization to muscle-adjacent regions does not require VAB-19, but the assembly of Myotactin into circumferential bands is dependent on VAB-19 (Fig. 5M). Myotactin is a large transmembrane protein with an extracellular domain consisting of ~32 fibronectin type-III repeats, suggesting that it could bind a ligand on muscle cells or muscle-associated extracellular matrix and thereby anchor attachment structures in muscle-adjacent regions. Unlike VAB-10A or intermediate filaments, the final localization of VAB-19 to attachment structures is completely dependent on Myotactin. VAB-19 might function in the Myotactin-dependent stabilization of attachment structures in muscle-adjacent regions; in the absence of Myotactin, VAB-19 would lose its association with attachment structures, and attachment structures lose their association with muscle.

The refinement of attachment structure localization into circumferential bands must involve interaction with CFBs. VAB-19 is not required for the segregation of attachment structures from actin CFBs, because attachment structures retain their striped appearance in *vab-19* mutants. However, VAB-19 could play a role in cross-talk between attachment structures and the cortical actin cytoskeleton. At present, the evidence for a specific interaction between VAB-19 and the actin cytoskeleton comes from the suppression of *vab-19* by *sma-1*. By analogy to other spectrins, SMA-1/β_H-spectrin probably cross-links apical actin and might stabilize integral membrane proteins within the apical epidermis (Dubreuil and Grushko, 1998). Is VAB-19 localized to the apical ends of attachment structures, consistent with a role in regulating the cortical actin cytoskeleton or SMA-1? Although epidermal attachment structures are too short to resolve apical versus basal localization, we can partly address this question by examining pharyngeal marginal cells, which contain longer attachment structures. In these cells, VAB-19::GFP appeared to be concentrated at the apical and basal ends of attachment structures. Although we do not know the role of *vab-19* in pharyngeal marginal cells, the similarities between pharyngeal and epidermal attachment structures suggest that, by analogy, VAB-19 might be present at the apical surface of the epidermis, consistent with a role in regulation of the cortical actin cytoskeleton. We infer from our genetic analysis that VAB-19 might locally inhibit or antagonize SMA-1 function, perhaps to allow attachment structures to move during the cell shape changes of epidermal elongation. Thus, in *sma-1* mutants, apical membrane proteins might be less highly cross-linked to cortical actin, partly bypassing the function of *vab-19*. Further tests of these models will require identification of proteins that interact with VAB-19.

Role of attachment structures in epidermal cell shape changes

Why are epidermal attachment structure components required for epidermal elongation? One model suggests that the function of attachment structures in elongation is indirect and reflects their role in muscle contraction. In mutants such as *vab-19*, muscles detach from the epidermis soon after muscle contraction begins, presumably because of a failure in the mechanical strength of epidermal muscle attachments. Muscle function is, for unknown reasons, required for epidermal elongation and so muscle detachment leads to elongation arrest. Alternatively, attachment structures might directly influence the organization of epidermal actin bundles, which are themselves required for elongation. Epidermal attachments and circumferential actin bundles are regularly interspersed in the muscle-adjacent parts of epidermal cells; during later stages, attachment structures are in register with the cuticular ridges known as annuli, whereas actin bundles coincide with the furrows separating annuli (Costa et al., 1997). The complementary distribution of actin CFBs and attachment structures suggests that they are mutually required for each other's organization. This is exemplified by VAB-10A/Plectin (an attachment-structure component) and VAB-10B/MACF, an actin-associated protein, which are mutually required for their organization into complementary circumferential bands (Bosher et al., 2003). The complementary pattern of actin and attachment structures arises gradually: actin and attachment structures might partly co-localize at early stages and only later segregate into alternating bands. Thus, the elongation defects of mutants defective in muscle might arise because muscles induce the development of epidermal attachment structures, which themselves influence the organization of epidermal actin.

What is the conserved cellular function of the VAB-19 family?

There are VAB-19 orthologs in the *Drosophila*, mouse, rat and human genomes. At present, however, little is known of the function of these VAB-19 family members. Based on the conservation of sequence in both the N-terminal motifs and the C-terminal ankyrin repeats, VAB-19 family members probably interact with conserved protein partners and function in regulating the cytoskeleton.

The *Drosophila* genome contains a single *vab-19* ortholog, whose function has not yet been determined. However, unlike *C. elegans*, *Drosophila* lacks cytoplasmic IFs (Fyrberg and Goldstein, 1990; Goldstein and Gunawardena, 2000). Instead, *Drosophila* muscle attachment structures contain microtubule (MT) bundles (Mogensen and Tucker, 1988). The *Drosophila* spectraplakin Shot (previously known as Kakapo) is a component of attachment structures and contains a MT-binding domain but not an IF-binding domain (Gregory and Brown, 1998; Röper et al., 2002). It will be important to determine whether the *Drosophila* VAB-19 is a component of MT-based muscle-attachment structures. The existence of a conserved VAB-19 family member in a species lacking cytoplasmic IFs further supports the hypothesis that VAB-19 does not interact directly with IFs. Nevertheless, VAB-19 and VAB-10-like spectraplakins could represent an evolutionarily conserved core of cell-matrix attachment structures.

The only vertebrate VAB-19 homolog for which functional data exist is the human gene *Kank*, which might function as a tumor suppressor for renal cell carcinoma, the most common malignancy of the adult kidney (Sarkar et al., 2002).

Expression of *Kank* in HEK293 cells suppressed cell growth and morphological changes, and expression of *Kank* in human kidney tumor (G-402) cells resulted in disorganization of actin (Sarkar et al., 2002). In light of the possible interaction of VAB-19 with actin in *C. elegans*, the VAB-19 family might play a conserved role in the actin cytoskeleton. The ability of human Kank partly to rescue *vab-19* mutant phenotypes supports the contention that the VAB-19 family has a conserved cellular function. It will clearly be informative to determine the subcellular localization and function of VAB-19 family members in vertebrate cells.

We thank J. Lewis for isolating *e1036*, S. George and R. Harrington for initial characterization of *e1036*, Y. Kohara for *vab-19* cDNAs, the Kazusa DNA Research Institute for the KIAA0172 cDNA clone, the *C. elegans* genome consortium for the sequences and cosmid DNAs, A. Fire for GFP vectors, and V. Praitis for her phalloidin staining protocol and SMA-1 antisera. We thank X. Huang, W.-M. Woo and N. Brown for discussions and comments on the manuscript. Some strains used here were obtained from the *Caenorhabditis* Genetics Center, which is supported by the NIH. YJ is an Assistant Investigator of the HHMI. This work was supported by a grant to ADC from the NIH (GM54657). The GenBank Accession Number for the *vab-19* cDNA sequence is AY273823

References

Albertson, D. G. and Thomson, J. N. (1976). The pharynx of *Caenorhabditis elegans*. *Philos. Trans. R. Soc. London Ser. B* **275**, 299-325.

Barstead, R. J. and Waterston, R. H. (1989). The basal component of the nematode dense-body is vinculin. *J. Biol. Chem*. **264**, 10177-10185.

Barstead, R. J. and Waterston, R. H. (1991). Vinculin is essential for muscle function in the nematode. *J. Cell Biol.* **114**, 715-724.

Bateman, A., Birney, E., Cerruti, L., Durbin, R., Etwiller, L., Eddy, S. R., Griffiths-Jones, S., Howe, K. L., Marshall, M. and Sonnhammer, E. L. (2002). The Pfam protein families database. *Nucleic Acids Res.* **30**, 276-280.

Bosher, J. M., Hahn, B.-S., Legouis, R., Sookhareea, S., Weimer, R. M., Gansmuller, A., Chisholm, A. D., Rose, A. M., Bessereau, J.-L. and Labouesse, M. (2003). The *C. elegans vab-10* spectraplakin isoforms protect the epidermis against internal and external forces. *J. Cell Biol.* **161**, 757-768.

Brenner, S. (1974). The genetics of *Caenorhabditis elegans*. *Genetics* **77**, 71-94.

Chin-Sang, I. D. and Chisholm, A. D. (2000). Form of the worm: genetics of epidermal morphogenesis in *C. elegans*. *Trends Genet.* **16**, 544-551.

Chin-Sang, I. D., George, S. E., Ding, M., Moseley, S. L., Lynch, A. S. and Chisholm, A. D. (1999). The ephrin VAB-2/EFN-1 functions in neuronal signaling to regulate epidermal morphogenesis in *C. elegans*. *Cell* **99**, 781-790.

Costa, M., Draper, B. W. and Priess, J. R. (1997). The role of actin filaments in patterning the *Caenorhabditis elegans* cuticle. *Dev. Biol*. **184**, 373-384.

Dubreuil, R. R. and Grushko, T. (1998). Genetic studies of spectrin: new life for a ghost protein. *BioEssays* **20**, 875-878.

Finney, M. and Ruvkun, G. (1990). The *unc-86* gene product couples cell lineage and cell identity in *C. elegans*. *Cell* **63**, 895-905.

Francis, R. and Waterston, R. H. (1991). Muscle cell attachment in *Caenorhabditis elegans*. *J. Cell Biol.* **114**, 465-479.

Fyrberg, E. A. and Goldstein, L. S. (1990). The *Drosophila* cytoskeleton. *Annu. Rev. Cell. Biol*. **6**, 559-596.

Gettner, S. N., Kenyon, C. and Reichardt, L. F. (1995). Characterization of β Pat-3 heterodimers, a family of essential integrin receptors in *C. elegans*. *J. Cell Biol.* **129**, 1127-1141.

Goldstein, L. S. and Gunawardena, S. (2000). Flying through the *Drosophila* cytoskeletal genome. *J. Cell Biol.* **150**, F63-68.

Gregory, S. L. and Brown, N. H. (1998). *kakapo*, a gene required for adhesion between and within cell layers in *Drosophila*, encodes a large cytoskeletal linker protein related to plectin and dystrophin. *J. Cell Biol.* **143**, 1271-1282.

Hallam, S. J., Goncharov, A., McEwen, J., Baran, R. and Jin, Y. (2002). SYD-1, a presynaptic protein with PDZ, C2 and RhoGAP-like domains, specifies axon identity in *C. elegans*. *Nat. Neurosci*. **5**, 1137-1146.

Hresko, M. C., Williams, B. D. and Waterston, R. H. (1994). Assembly of body wall muscle and muscle cell attachment structures in *Caenorhabditis elegans*. *J. Cell Biol.* **124**, 491-506.

Hresko, M. C., Schriefer, L. A., Shrimankar, P. and Waterston, R. H. (1999). Myotactin, a novel hypodermal protein involved in muscle-cell adhesion in *Caenorhabditis elegans*. *J. Cell Biol.* **146**, 659-672.

Karabinos, A., Schmidt, H., Harborth, J., Schnabel, R. and Weber, K. (2001). Essential roles for four cytoplasmic intermediate filament proteins in *Caenorhabditis elegans* development. *Proc. Natl. Acad. Sci. USA* **98**, 7863-7868.

Köppen, M., Simske, J. S., Sims, P. A., Firestein, B. L., Hall, D. H., Radice, A. D., Rongo, C. and Hardin, J. D. (2001). Cooperative regulation of AJM-1 controls junctional integrity in *Caenorhabditis elegans* epithelia. *Nat. Cell. Biol*. **3**, 983-991.

Maeda, I., Kohara, Y., Yamamoto, M. and Sugimoto, A. (2001). Large-scale analysis of gene function in *Caenorhabditis elegans* by high-throughput RNAi. *Curr. Biol*. **11**, 171-176.

Mango, S. E. (2001). Stop making nonSense: the *C. elegans smg* genes. *Trends Genet.* **17**, 646-653.

McKeown, C., Praitis, V. and Austin, J. (1998). *sma-1* encodes a β_H-spectrin homolog required for *Caenorhabditis elegans* morphogenesis. *Development* **125**, 2087-2098.

Mello, C. C., Kramer, J. M., Stinchcomb, D. and Ambros, V. (1991). Efficient gene transfer in *C. elegans*: extrachromosomal maintenance and integration of transforming sequences. *EMBO J.* **10**, 3959-3970.

Mogensen, M. M. and Tucker, J. B. (1988). Intermicrotubular actin filaments in the transalar cytoskeletal arrays of *Drosophila*. *J. Cell Sci.* **91**, 431-438.

Norman, K. R. and Moerman, D. G. (2002). Alpha spectrin is essential for morphogenesis and body wall muscle formation in *Caenorhabditis elegans*. *J. Cell Biol.* **157**, 665-677.

Piekny, A. J., Wissmann, A. and Mains, P. E. (2000). Embryonic morphogenesis in *Caenorhabditis elegans* integrates the activity of LET-502 Rho-binding kinase, MEL-11 myosin phosphatase, DAF-2 insulin receptor and FEM-2 PP2c phosphatase. *Genetics* **156**, 1671-1689.

Priess, J. R. and Hirsh, D. I. (1986). *Caenorhabditis elegans* morphogenesis: the role of the cytoskeleton in elongation of the embryo. *Dev. Biol*. **117**, 156-173.

Röper, K., Gregory, S. L. and Brown, N. H. (2002). The 'spectraplakins': cytoskeletal giants with characteristics of both spectrin and plakin families. *J. Cell Sci.* **115**, 4215-4225.

Sambrook, J. and Russell, D. (2001). *Molecular Cloning: A Laboratory Manual*. Cold Spring Harbor, New York: Cold Spring Harbor Laboratory Press.

Sarkar, S., Roy, B. C., Hatano, N., Aoyagi, T., Gohji, K. and Kiyama, R. (2002). A novel ankyrin repeat-containing gene (*Kank*) located at 9p24 is a growth suppressor of renal cell carcinoma. *J. Biol. Chem*. **277**, 36585-36591.

Schwarz-Romond, T., Asbrand, C., Bakkers, J., Kuhl, M., Schaeffer, H. J., Huelsken, J., Behrens, J., Hammerschmidt, M. and Birchmeier, W. (2002). The ankyrin repeat protein Diversin recruits casein kinase Iε to the β-catenin degradation complex and acts in both canonical Wnt and Wnt/JNK signaling. *Genes Dev.* **16**, 2073-2084.

Sedgwick, S. G. and Smerdon, S. J. (1999). The ankyrin repeat: a diversity of interactions on a common structural framework. *Trends Biochem. Sci*. **24**, 311-316.

Simske, J. S. and Hardin, J. (2001). Getting into shape: epidermal morphogenesis in *Caenorhabditis elegans* embryos. *BioEssays* **23**, 12-23.

Williams, B. D. and Waterston, R. H. (1994). Genes critical for muscle development and function in *Caenorhabditis elegans* identified through lethal mutations. *J. Cell Biol.* **124**, 475-490.

Wissmann, A., Ingles, J., McGhee, J. D. and Mains, P. E. (1997). *Caenorhabditis elegans* LET-502 is related to Rho-binding kinases and human myotonic dystrophy kinase and interacts genetically with a homolog of the regulatory subunit of smooth muscle myosin phosphatase to affect cell shape. *Genes Dev.* **11**, 409-422.

Wissmann, A., Ingles, J. and Mains, P. E. (1999). The *Caenorhabditis elegans mel-11* myosin phosphatase regulatory subunit affects tissue contraction in the somatic gonad and the embryonic epidermis and genetically interacts with the Rac signaling pathway. *Dev. Biol*. **209**, 111-127.